the plant journal

SEB Society for Experimental Biology

The Plant Journal (2013) **74,** 280–293 doi: 10.1111/tpj.12120

The *cis*-acting CTTC–P1BS module is indicative for gene function of *LjVTI12*, a Qb-SNARE protein gene that is required for arbuscule formation in *Lotus japonicus*

Frédéric Lota[1], Sarah Wegmüller[2,†], Benjamin Buer[1], Shusei Sato[3], Andrea Bräutigam[4], Benjamin Hanf[1] and Marcel Bucher[1,*]

[1]*Botanical Institute, Cologne Biocenter, Cluster of Excellence on Plant Sciences, University of Cologne, Zülpicherstraße 47b, D-50674, Cologne, Germany,*

[2]*Institute of Agricultural Sciences, Federal Institute of Technology Zurich, Experimental Station Eschikon 33, CH-8315, Lindau, Switzerland,*

[3]*Laboratory of Plant Genes, Kazusa DNA Research Institute, Kisarazu, Chiba, 292-0812, Japan, and*

[4]*Plant Biochemistry, Heinrich Heine University, Universitätsstraße 1, D-40225, Düsseldorf, Germany*

Received 24 November 2012; revised 08 January 2013; accepted 14 January 2013; published online 2 March 2013.

*For correspondence (e-mail m.bucher@uni-koeln.de).

†Present address: Institute of Life Technologies, University of Applied Sciences Western Switzerland, Route du Rawyl 64, CH-1950, Sion,Switzerland.

SUMMARY

The majority of land plants live in symbiosis with arbuscular mycorrhizal fungi from the phylum Glomeromycota. This symbiosis improves acquisition of phosphorus (P) by the host plant in exchange for carbohydrates, especially under low-P availability. The symbiosome, constituted by root cortex cells accommodating arbuscular mycorrhizal fungal hyphae, is the site at which bi-directional exchange of nutrients and metabolites takes place. Uptake of orthophosphate (Pi) in the symbiosome is facilitated by mycorrhiza-specific plant Pi transporters. Modifications of the potato Pi transporter 3 (*StPT3*) promoter were analysed in transgenic mycorrhizal roots, and it was found that the CTTC *cis*-regulatory element is necessary and sufficient for a transcriptional response to fungal colonization under low-Pi conditions. Phylogenetic footprinting also revealed binary combination of the CTTC element with the Pi starvation response-associated PHR1-binding site (P1BS) in the promoters of several mycorrhiza-specific Pi transporter genes. Scanning of the *Lotus japonicus* genome for gene promoters containing both *cis*-regulatory elements revealed a strong over-representation of genes involved in transport processes. One of these, *LjVTI12*, encoding a member of the SNARE family of proteins involved in membrane transport, exhibited enhanced transcript levels in *Lotus* roots colonized with the arbuscular mycorrhizal fungus *Glomus intraradices*. Down-regulation of LjVTI12 by RNA interference resulted in a mycorrhiza-specific phenotype characterized by distorted arbuscule morphology. The results highlight cooperative *cis*-regulation which integrates mycorrhiza and Pi starvation signaling with vesicle trafficking in symbiosome development.

Keywords: *Lotus japonicus*, *Solanum tuberosum*, arbuscular mycorrhiza, P1BS, SNARE, intracellular trafficking.

INTRODUCTION

Mycorrhizal symbiosis is thought to have evolved over 460 million years ago, and was important for the colonization of land by plants (Remy *et al.*, 1994; Redecker *et al.*, 2000). Development of the symbiosome, which is the major site of mutual exchange of nutrients and metabolites between the symbionts, is of special interest in understanding the function of arbuscular mycorrhizae (AM) (Bucher, 2007). A promising target for studying and understanding the fundamental mechanisms underlying symbiosome formation are the mycorrhiza-inducible orthophosphate (Pi) transporters of the Pht1 family that are transcriptionally regulated in cortex cells accommodating fungal arbuscules or hyphal coils (Rausch *et al.*, 2001; Harrison *et al.*, 2002; Karandashov *et al.*, 2004). The first mycorrhiza-inducible Pi transporter described was StPT3 (*Solanum tuberosum* phosphate transporter 3) from potato. A 1.7 kb region of its gene promoter was shown to direct mycorrhiza-inducible expression of reporter genes

exclusively in cells containing arbuscules and hyphal coils (Rausch *et al.*, 2001; Karandashov *et al.*, 2004; Nagy *et al.*, 2005). Further studies subsequently proposed that expression of *StPT3* and related mycorrhizal genes is controlled by a Pi-dependent repression/de-repression mechanism that is similar to the Pi starvation response regulation mechanism in solanaceous species (Nagy *et al.*, 2009; Breuillin *et al.*, 2010). Moreover, roots from high Pi-treated plants became insensitive to a mycorrhizal signal that triggers *StPT3* expression under low-Pi conditions (Drissner *et al.*, 2007; Nagy *et al.*, 2009). Inspection of the *StPT3* promoter sequence revealed putative binding sites for transcription factors, one of which, with the sequence **CTTC**TTGTTCTA, was named the CTTC element for simplicity (Karandashov *et al.*, 2004). Overall, these findings suggest multi-level transcriptional regulation of mycorrhiza-inducible Pi transporters.

During the process of arbuscule development, the plant cellular membrane expands approximately 10-fold (Alexander *et al.*, 1989) in order to completely surround the arbuscule, thus forming the peri-arbuscular membrane. Although the peri-arbuscular membrane is continuous with the peripheral plasma membrane of the cell, asymmetric distribution of transport proteins has been demonstrated, suggesting intense trafficking of cellular membrane components, membrane proteins and cell-wall precursors to the extending peri-arbuscular membrane (Harrison *et al.*, 2002, 2010; Bucher, 2007). This membrane is therefore a major component of the symbiosome, and participates in the exchange of nutrients and metabolites between the symbionts. Research into plant–microbe interactions has indicated that cytoskeletal rearrangements after microbial attack in the host cell are accompanied by site-directed secretion of proteins and/or natural products (Osbourn *et al.*, 2006). For example, a vesicle-associated and soluble *N*-ethylmaleimide-sensitive factor attachment protein receptor (SNARE) protein-mediated exocytosis pathway appears to drive focal secretion of antimicrobial cargo into the apoplastic space during the immune response against pathogenic fungi (Kwon *et al.*, 2008). Furthermore, intense intracellular trafficking of cellular compounds must occur during formation of the pre-penetration apparatus that is formed during efficient epidermal penetration by AM fungi and arbuscule formation in the cortex of plant roots. Pre-penetration apparatus formation involves aggregation of cytoskeletal elements and repositioning of the nucleus, endoplasmic reticulum and Golgi apparatus, and probably involves the targeting of vesicles to the site of microbial entry (Genre *et al.*, 2005; Hardham *et al.*, 2007; Ivanov *et al.*, 2010). In this paper, the presence of two *cis*-regulatory elements (CREs) in the *StPT3* promoter and their subsequent functional characterization in potato and *Lotus japonicus* suggest convergence of the mycorrhiza and Pi signaling pathways in the regulation of symbiosome development. Both CREs, when used as targets for genome scanning in *L. japonicus*, led to the identification of mycorrhiza up-regulated genes, including the SNARE-encoding gene *LjVTI12*, which, through use of RNAi, was shown to be involved in arbuscule formation.

RESULTS AND DISCUSSION

StPT3 promoter dissection reveals a putative CRE important for mycorrhiza-specific gene regulation

A 1727 bp *StPT3* promoter sequence (Figure S1) was previously shown to direct β-glucuronidase (GUS) reporter gene expression to root cells containing arbuscules or hyphal coils (Rausch *et al.*, 2001; Karandashov *et al.*, 2004). To identify regulatory sequences involved in mycorrhiza-specific *StPT3* expression, a series of 5′ deletions of the *StPT3* promoter were fused to the GUS reporter gene (Figure 1a, b) in the binary vector BIN 19 (Bevan, 1984). These constructs were introduced into *Agrobacterium rhizogenes*, and then used to generate composite plants with non-isogenic transgenic hairy roots, which were subsequently colonized with the AM fungus *Glomus intraradices* (synonym *Rhizophagus irregularis*). Previous studies have shown that the hairy roots of host plants are colonized by AM fungi in the same way as wild-type roots (Hause *et al.*, 2009). Mycorrhizal roots containing the *−1727::GUS* chimeric gene (Figure 1a and Figure S2) showed strong GUS activity, as shown in Rausch *et al.* (2001), and were used as a positive control for qualitative assessment of promoter activity in the deletion constructs. The *−1220*, *−1052* and *−640* promoter fragments, respectively, were still able to confer GUS activity. However, microscopic analysis indicated an absence of GUS expression in colonized hairy roots carrying the *−511*, *−298*, *−201* and *−135* promoter fragments. This suggests the presence of a regulatory region for *StPT3* expression within the 129 bp fragment from −640 to −511 bp upstream of the start ATG (Figure 1b and Figure S2). To test whether the 129 bp fragment contains CREs that are sufficient for mycorrhiza-specific activity, it was fused upstream of the 35S minimal promoter::*GUS* (*129mini::GUS*) construct (Figure 1c). The minimal promoter contains only the TATA box and the transcription start site, which determine the direction of gene transcription, but requires the addition of CREs to direct a spatio-temporal expression pattern (Benfey *et al.*, 1989). Mycorrhizal hairy roots carrying the *129mini::GUS* construct exhibited strong GUS activity that co-localized with mycorrhizal structures (Figure 1c and Figure S2). This demonstrates that the 129 bp fragment is sufficient to confer mycorrhiza-specific activity to the *StPT3* gene promoter (see also Karandashov *et al.*, 2004). The hairy roots used in these studies were generally well colonized by *G. intraradices*. This *StPT3* promoter deletion analysis (Figure 1a,b) indicated that neither a previously proposed putative HD-Zip-1 binding site

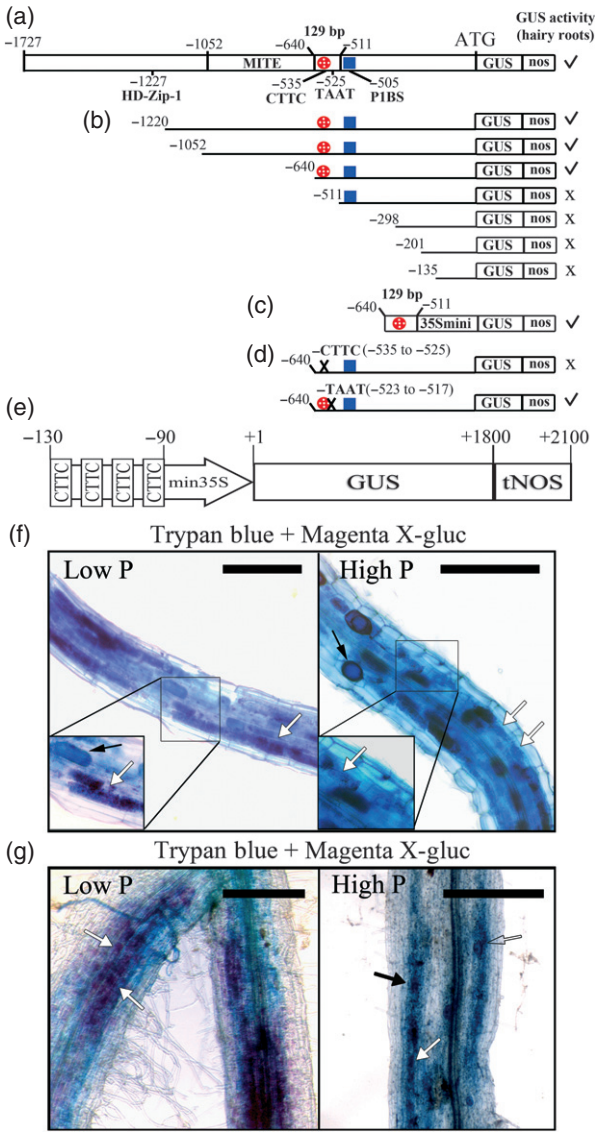

Figure 1. *StPT3* promoter deletion constructs and their activity in mycorrhizal potato and *Lotus* hairy roots.

(a) *StPT3* promoter and location of the MITE, HD-Zip-1 and regulatory *cis*-elements CTTC, TAAT and P1BS.

(b) Effect of *StPT3* promoter truncations fused to the β-glucuronidase gene (GUS) and the nopaline synthase (nos) terminator on activity in mycorrhizal potato hairy roots.

(c) A 129 bp fragment of the *StPT3* promoter fused to the CaMV 35S minimal promoter (35Smini) and GUS (*129mini::GUS*). (d) *StPT3* promoter::GUS fusions (640 bp) carrying a deletion of the CTTC motif (*−CTTC::GUS*) or the TAAT motif (*−TAAT::GUS*).

For (a–d), tick symbols indicate that GUS activity co-localized with arbuscular mycorrhizal fungus structures, while crosses indicate that GUS activity does not co-localize with arbuscular mycorrhizal fungus structures. Red circles represent the CTTC motif and blue squares represent the P1BS motif.

(e) Synthetic promoter consisting of a quadruple tandem repeat of the CTTC motif fused to β-glucuronidase (GUS) and the nopaline synthase terminator (tNOS).

(f) Activity of the construct shown in (e) in mycorrhizal potato hairy roots under low-Pi (left) or high-Pi (right) conditions.

(g) Activity of the construct shown in (e) in mycorrhizal *Lotus* hairy roots under low-Pi (left) or high-Pi (right) conditions.

Scale bars = 0.5 mm (f, g). The white and black arrows in (f) and (g) indicate arbuscules/coils and vesicles, respectively.

nor a MITE element (Rausch *et al.*, 2001) are required for the mycorrhiza-inducible expression of *StPT3*.

Phylogenetic footprinting is a method that sifts conserved motifs in non-coding regions of orthologous genes of various species. Six putative CREs, including TAAT and CTTC (see below), have previously been identified within promoters of four mycorrhiza-inducible Pi transporter genes [from potato, tomato (*Solanum lycopersicum*), *Medicago* and rice (*Oryza sativa*)] using phylogenetic footprinting. In *StPT3*, they clustered within the 129 bp promoter fragment, which previously led us to speculate on their involvement in mycorrhiza-dependent up-regulation of *StPT3* (Karandashov *et al.*, 2004). Mycorrhizal-*CTTC::GUS*-carrying roots always lacked GUS activity (Figure 1d and Figure S2), thus authenticating this previously identified CTTC motif (Karandashov *et al.*, 2004) as a CRE involved in mycorrhizal *StPT3* gene regulation. In contrast, deletion of the other five putative CREs, including the TAAT motif, present in the 129 bp fragment produced GUS expression levels equal to that of the *−640::GUS* lines, eliminating these motifs as candidate CREs (Figure 1d and Figure S2). Furthermore, to test the importance of the CTTC motif in the 1.7 kb *StPT3* promoter, transgenic potato plants were generated that express β-glucuronidase under the control of the 1.7 kb *StPT3* promoter in which a CTTCTTGTTC deletion in the CTTC motif was introduced. Roots from transgenic potato plants (Δ*CTTC* in *promStPT3*, Figure S3) were stained for GUS and were compared to the *promStPT3* (1.7 kb) line. As shown in Figure S3A, only 13% of analyzed root sections showed GUS signals in the Δ*CTTC* line compared to 78% in the *promStPT3* line. All plants were equally colonized with *G. intraradices*. Quantitative GUS analysis was then performed using total protein extracts from mycorrhizal roots, and showed similar results (Figure S3B). A strong reduction in GUS activity was observed in the *ΔCTTC-promStPT3* line, which exhibited GUS activity near background levels of the wild-type control. Taken together, it may be concluded that the CTTC element is essential for the regulation of mycorrhizal *StPT3* promoter activity in potato roots.

An alignment of the potato CTTC element (TCCTTCT TGTTCTA) and its flanking regions with the corresponding sequences in all 14 mycorrhizal Pi transporter gene promoters studied here led to identification of the core CTTC motif (TCTTGTT, with the exception of *OsPT11*, where the third T is replaced by a C; Table 1). Most dicot genes encoding mycorrhiza-specific Pi transporters from the Pht1 sub-family I (Nagy *et al.*, 2005) were shown to contain the conserved core sequence TCTTGTT within the same sub-region of the corresponding promoter, 100–200 bp upstream of the start ATG (Figure 2 and Table 1). Interestingly, the CTTC element in *PhPT3*, which encodes a Pht1 sub-family II protein, is found within the same sub-region as in Pht1 sub-family I genes, while the motif in the closely

Table 1 CTTC elements in various plant promoters

Gene	Promoter length (bp)	Gene type	Position	Motif sequence	References
PhPT3	1000	myc PT	−97	ctTg**TCTTGTTC**Tg	Bucher *et al.* (2008)
StPT3	1000	myc PT	−535	tccT**TCTTGTTC**Ta	Rausch *et al.* (2001)
PhPT4	631	myc PT	−129	aaTT**TCTTGTTC**Ta	Bucher *et al.* (2008)
PhPT5	1000	myc PT	−156	aaTT**TCTTGTTC**Ta	Bucher *et al.* 2008
LePT4	869	myc PT	−137	aaTT**TCTTGTTC**Ta	Nagy *et al.* (2005)
StPT4	1000	myc PT	−139	aaTT**TCTTGTTC**Ta	Nagy *et al.* (2005)
MtPT4	865	myc PT	−174	ttTT**TCTTGTTC**Tc	Harrison *et al.* (2002)
OsPT13	1000	myc PT	−793	acTT**TCTTGTTC**ct	Paszkowski *et al.*, 2002;
PhPT4	631	myc PT	−628	caTT**TCTTGTT**acc	Bucher *et al.* (2008)
MtGST1	876	myc	−865	atTT**TCTTGTT**aga	Krajinski *et al.* (2003)
ENOD12B	1000	myc	−867	ttTT**TCTTGTT**tgc	Hansen *et al.* (1999)
AtPT1	1000	PT	−177	gtTT**TCTTGTTC**at	Mudge *et al.* (2002)
MtSCP1	1000	myc	−118	taaca**CTTGTT**tca	Harrison *et al.* (2003)
MtCEL1	1000	myc	−594	ttTT**TCTT**c**TTC**Tt	Harrison *et al.* (2003)
PhPT3	1000	myc PT	−632	ttTT**TCTT**c**TT**tcg	Bucher *et al.* (2008)
OsPT11	1000	myc PT	−157	gccc**TC**T**c**G**TTC**at	Paszkowski *et al.* (2002)
LjPT3	2000	myc PT	−12	gat**TTCTTGTTC**ctt	Guether *et al.* (2009)
LjPT4	1400	myc PT	−131	tccT**TCTTGTTC**aca	Guether *et al.* (2009)
Consensus				hhTT**TCTTGTTC**Tn	

The extended element is shown in capital letters, and the core element is shown in bold letters. Deviations from the consensus element TCTTGTTC are indicated in lower-case letters. myc PT; mycorrhiza-specific phosphate transporter.

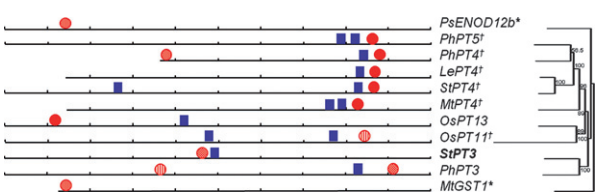

Figure 2. Phylogenetic footprinting of AM-induced genes.
(a) Phylogenetic footprinting for mycorrhiza-inducible Pi transporter-encoding genes and other mycorrhiza-inducible genes. The lines with 100 bp intervals represent promoter fragments of 1000 bp or less. The phylogram represents the corresponding coding sequences. Numbers on the tree represent bootstrap values. Red circles represent the CTTC motif and blue squares represent the P1BS motif. Filled shapes represent a 100% match to the extended motif present (TT**TCTTGTTC**T). Spotted shapes represent motifs that only match the core motif; hatched shapes represent motifs with base pair changes in the core motif. The dagger symbol (†) indicates mycorrhiza-inducible genes encoding mycorrhizal Pi transporters of Pht1 sub-family I; asterisks indicate AM-inducible genes encoding proteins other than Pi transporters.

related *StPT3* gene is located in a different sub-region (Figure 2). With the exception of *AtPT1* (Table 1), the CTTC motif is absent in the promoter regions of the *Pht1* members of Arabidopsis, which coincideS with the status of the Brassicaceae as non-mycorrhizal species. Similarly, the CTTC motif is absent in the promoter regions of mycorrhiza-independent rice *Pht1* family members. Moreover, the CTTC element was also found in the promoters of unrelated mycorrhiza-inducible genes from legume species with some sequence variation, i.e. in the mycorrhiza-inducible *PsENOD12b*, *MtGst1*, *MtCEL1* and *MtSCP1* genes, but not in *VfLb29* (Figure 2 and Table 1). Overall, these data suggest that the CTTC motif is a mycorrhizal CRE, the function of which is conserved in a subset of mycorrhiza-inducible genes involved in symbiosome development and nutrient uptake, thus transcending mycorrhiza-specific Pi transporter genes.

The CTTC element is necessary and sufficient for mycorrhiza-specific GUS expression in Pi-starved potato and *Lotus* roots

To further investigate the role of the CTTC element in gene regulation, and possible control of CTTC by Pi repression (Nagy *et al.*, 2009; Breuillin *et al.*, 2010), four tandem CTTC repeats were fused to a 35S minimal promoter upstream of the GUS gene (Figure 1e). The chimeric gene was subsequently cloned into the binary vector pRedRoot containing the constitutively expressed fluorescent protein DsRED1 (Limpens *et al.*, 2004). Transgenic *A. rhizogenes*-transformed potato and *Lotus* hairy roots exhibited red fluorescence and could thus be distinguished from non-fluorescent wild-type roots growing on the same composite plant. A combination of histochemical staining using Magenta-β-D-glucuronide cyclohexylammonium salt (Biosynth, Basel), http://www.biosynth.com/) as the GUS substrate and Trypan blue was subsequently performed as described previously (Karandashov *et al.*, 2004; Nagy *et al.*, 2005). This demonstrated co-localization of GUS activity and fungal colonization in mycorrhizal root sectors of both plant species (Figure 1f,g, left, white arrows). Moreover, weak magenta staining was observed in cells containing hyphal coils, but not in root cells containing vesicles (black arrows). This indicates that the CTTC element is both necessary and sufficient for mycorrhiza-specific gene

regulation in root cells harboring arbuscules or hyphal coils under low-Pi conditions. After addition of 1 mM $NH_4H_2PO_4$ to mycorrhizal potato plants or 5 mM $NH_4H_2PO_4$ to mycorrhizal *Lotus* plants, GUS staining became undetectable in cells containing developed arbuscules (Figure 1f,g, right, white arrows) or hyphal coils (black arrow). This indicated repression of CTTC-mediated *cis*-regulation of gene expression in colonized cells by a postulated Pi repression mechanism.

Cooperative function proposed for the two CREs, CTTC and P1BS, in response to mycorrhiza formation

Analysis of 11 AM-inducible genes and their promoters (i.e. the region up to 1 kb upstream of the start codon, ATG) has narrowed the number of conserved motifs compared to the previous study (Karandashov *et al.*, 2004), and led to identification of the Pi starvation-associated P1BS element with the consensus sequence GnATATnC (Rubio *et al.*, 2001) 30 bp downstream of CTTC motif (Figures 1 and 2) and adjacent to the 129 bp element (Figure 1b,d). Chen *et al.* (2011) suggested that the activity of a CTTC-like motif (MYCS) depends on the activity of P1BS and probably other CREs involved in mycorrhiza-specific gene regulation in tobacco. In contrast, our work indicated that CTTC alone is an integrator CRE of mycorrhizal and Pi repression signaling, independent of P1BS. Therefore, although the co-localization of P1BS and CTTC suggested a function of both CREs in mycorrhiza-specific Pi transporter gene regulation, the role of P1BS is still ambiguous. Interestingly, the mycorrhiza-specific Pi transporter gene *LjPT4* from *L. japonicus* also contained the two CREs with similar spacing (Table 2). To study whether the concurrent presence of CTTC and P1BS is indicative of gene expression in response to mycorrhiza formation, a motif-based profile scanning approach was performed with *L. japonicus* to obtain a genome-wide prediction of genes that are likely to be regulated in a similar way as *StPT3*. These genes may be involved in symbiosome development and/or function. The *L. japonicus* genome has been sequenced to an extent of >67%, covering over 91% of the gene space (Sato *et al.*, 2008). The available *Lotus* genome sequence was scanned using features based on the sequence of the CREs and the distance between them (16–22 nt) and the number of mismatches (a maximum of three) (search sequence was TTCTTGTTCN(16,22)G[AG]ATAT[ACT]C). A total of 10 082 hits were annotated as retro-elements and pseudogenes (25 and 20% of total hits, respectively), or partial (19%), expressed sequence tags (EST) (6%) and full gene sequences (38%). A total of 4634 sequences contained both motifs upstream (maximum 2100 nucleotides) of their corresponding start ATG. These *Lotus* gene sequences were then compared to the Arabidopsis genome by reciprocal BLAST analysis (Moreno-Hagelsieb and Latimer, 2008). Functional classification revealed strong over-representation of genes involved in cellular transport processes (Figure 3a). A detailed functional class analysis of transporter genes containing CTTC and P1BS motifs with one to three mismatches in their promoters is shown in Figure 3(b) (red

Table 2 Expression analysis by quantitative RT-PCR of *Lotus* candidate 'symbiosome genes' involved in transport mechanisms containing both CREs, CTTC and P1BS, with up to three mismatches

Gene accession	Possible function	Quantitative RT-PCR	CRE sequence (distance to downstream CDS in nt)
chr3_CM0208_260_r2	Cation efflux transporter/zinc transporter	1.85 ± 0.44 2.61 ± 0.32 2.02 ± 0.27	TCTTGTTTCTATTTAATGCTTAGAAGAATGTTT (62)
chr1.CM0141.500.nd	Vesicle transport (LjVTI12)	7.35 ± 1.1 6.9 ± 1.2 0.46 ± 0.05	ACTTGTCGCAGAAAAGTGTTGTATACAAGAATATTC (197)
chr1_CM0036_250_r2	Amino acid/polyamine transporter	2.33 ± 0.3 0.96 ± 0.16 1.96 ± 0.24	TCTTGGTCAACATGGTGCTATGCTAAGGATATTG (1135)
chr3_CM0792_290_r2	Cation efflux transporter/zinc transporter	1.64 ± 0.32 1.24 ± 0.36 3.8 ± 0.38	TGTTGTTAGCAGCTGACTCTGCCCCCTTGGATATTC (358)
chr3_CM0160_30_r2	Sugar transporter	3.56 ± 1.12 2.7 ± 0.53 0.75 ± 0.27	TCATGTTCATGAGCTGCGATATGTTAAAGGAATTTC (403)
chr4_CM0244_740_r2	Ca^{2+}-transporting ATPase	2.1 ± 0.4 1.81 ± 0.46	TCTTGATCATGTACTATGTGTTGCTTGTTAATTTAC (876)
LjT24M05_60_r2	Oligopeptide transporter-like	3.73 ± 0.83 1.68 ± 0.32	TGTTTTGCACTCCACACTTTTAGAGGAATATAC (1122)
chr1_CM2121_10_r2	Phosphate transporter 4	Mycorrhiza-specific	TCTTGTTCACATCTCCTAAACTTAGGACTACAC (107)

Relative expression values are represented as fold change in mycorrhizal versus non-mycorrhizal RNA samples. The mean values ± SE of three technical replicates for each of two biological samples (mycorrhizal and non-mycorrhizal) of two or three independent experiments are shown, except for the Pi transporter 4 gene which is specifically induced in mycorrhizae.

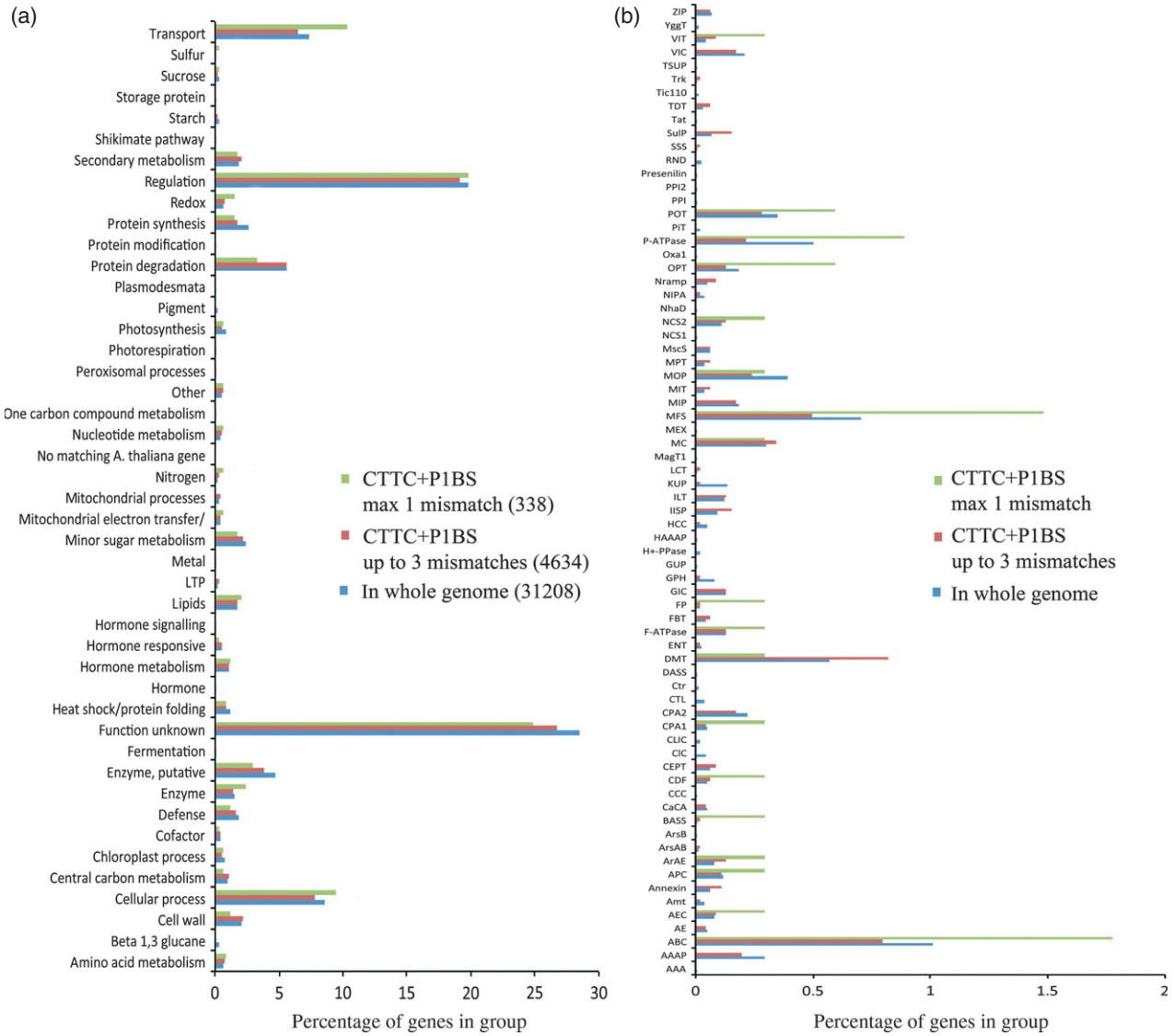

Figure 3. BLAST analysis and functional classes of *Lotus* genes containing both CREs (CTTC and P1BS).
(a) A BLAST search was performed using *Lotus* genes containing both CREs against the Arabidopsis genome, and the genes were classified into functional groups. Blue bars represent the abundance of the gene class compared to all known Arabidopsis genes. Red bars represent the abundance of genes from one class containing both CREs with up to three mismatches. Green bars represent the abundance of genes from one class containing both CREs with up to one mismatch. Numbers in parentheses are the total number of genes.
(b) Detailed view of the functional transporter gene class represented in (a) with the same color code.

and green bars, respectively). This sub-classification showed a strong over-representation of members of the major facilitator super-family (MFS) and the ATP-binding cassette (ABC) super-family, implicating combined CTTC and P1BS elements in transcriptional regulation of members of these gene families. For further gene expression analysis by real-time RT-PCR, 49 genes were selected that were proposed to be involved in transport processes, including genes that may play a role in subcellular targeting of transporter and other membrane proteins. Total RNA extracted from Pi-starved mycorrhizal or non-mycorrhizal roots was subjected to gene expression analysis using gene-specific primer pairs. Of the 49 genes (see Table S1), 11 candidate genes were initially suggested to be induced by mycorrhizal colonization with a threshold value of ≥ 2 in a single plant. Subsequently, eight genes showed consistent up-regulation in symbiotic roots in two to three biological replicates (Table 2). This included two genes encoding putative zinc transporters from the cation efflux transporter family (Table 2), consistent with studies showing enhanced amounts of Zn in mycorrhizal plant shoots (Hamel *et al.*, 2000). The identification of putative amino acid/polyamine transporter-encoding genes suggests a role for the expressed proteins in polyamine homeostasis in the symbi-

osome. Polyamines were shown to have positive effects on colonization frequency (Elghachtouli *et al.*, 1995), and were proposed to play a role in Pi nutrition-dependent regulation of AM symbiosis (Paradi *et al.*, 2003). Similarly, expression of an oligopeptide transporter-like gene was enhanced upon mycorrhization, supporting previous studies on fungal effector peptides that participate in fungal colonization (Kloppholz *et al.*, 2011). Expression of a calcium-transporting ATPase was also identified as AM-enhanced. Two MFS genes showed differential levels of expression upon mycorrhization, i.e. the *LjPT4* gene showed expression restricted to mycorrhizal *Lotus* roots as shown previously (Guether *et al.*, 2009), while a sugar transporter gene exhibited enhanced expression after mycorrhizal colonization. A gene encoding a member of the SNARE fusion complex superfamily involved in intracellular vesicle trafficking (Surpin *et al.*, 2003; Ungar and Hughson, 2003) was also identified by this *in silico* approach. This protein was of special interest because it may be involved in cell sorting of membrane components to the extending peri-arbuscular membrane. The mycorrhiza-dependent expression was variable (0.46–7.35-fold induction), suggesting fine regulation via the presence and/or biological activity of AM fungal structures as previously proposed for the *StPT3* gene (Karandashov *et al.*, 2004).

According to Guether *et al.* (2009), approximately 1% of *Lotus* genes are mycorrhiza-inducible (558 of 50 864). This subset of eight of 49 mycorrhiza-regulated genes accounts for 16% of validated motif-containing genes. Statistical analysis using Fisher's exact test showed an over-representation of mycorrhiza-regulated genes in the set (compared to 585 of 50 864), with a *P* value of 0.0017, which is highly significant. Taken together, these results suggest cooperative regulatory roles for CTTC and P1BS in expression of genes that are likely to be involved in symbiosome development and/or function.

The mycorrhiza-regulated SNARE protein LjVTI12 is involved in arbuscule development

Two major processes involved in symbiosome development and functioning are trafficking of membrane constituents (such as transport proteins and lipids) to the extending peri-arbuscular membrane, and recycling of peri-arbuscular membrane material during arbuscule degradation. Little is currently known about these mechanisms, which are likely to involve intracellular trafficking, secretion and vesicular transport processes. Vesicle trafficking is well described in Arabidopsis, which is unable to form AM. It involves many genes whose encoded proteins mediate highly specific targeted vesicle fusion (Uemura *et al.*, 2004). Vapyrin, a vesicle-associated membrane protein (VAMP), was shown to be involved in cellular remodeling during AM symbiosis (Harrison *et al.*, 2010). One of the genes induced by mycorrhizal colonisation and carrying the putative CTTC/P1BS regulatory module in their promoter was the predicted gene with the accession chr1.CM0141.540 (Table 2), which encodes a SNARE protein. This protein is thus a likely component of the core machinery of membrane fusion vesicle-associated proteins implicated in *Lotus* AM symbiosis. The protein shares 58.6% sequence identity (Pearson *et al.*, 1997) with the Arabidopsis SNARE protein AtVTI12, which has been suggested to be involved in plant autophagy under poor nutrient conditions (Surpin *et al.*, 2003). Phylogenetic comparison classified both proteins to the Qb-SNARE family of vesicle-docking proteins carrying the Qb-SNARE motif in their C-terminus (Figure 4a). Therefore, the *Lotus* gene was

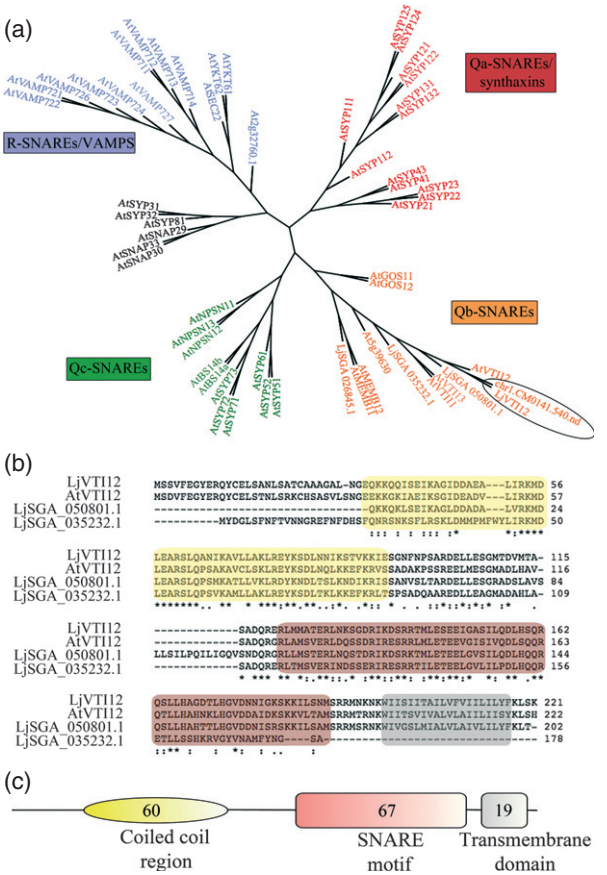

Figure 4. Phylogeny and protein sequence analysis of *Lotus* chr1.CM0141.500.nd.

(a) Unrooted phylogenetic tree of Arabidopsis SNAREs including the *Lotus* protein chr1.CM0141.540.nd (encircled) and its closest homologs LjSGA_050801.1, LjSGA_035232.1 and LjSGA_026845.1, suggesting that they are members of the Qb-SNARE protein family. The name LjVTI12 was given to chr1.CM0141.540.nd due to its homology to Arabidopsis AtVTI12.

(b) *LjVTI12* encodes a protein of 221 amino acids containing three conserved domains. The conserved coiled-coil domain is highlighted in yellow and is located at the N-terminus of the protein. The conserved SNARE motif (67 amino acids) is highlighted in pink. The transmembrane domain is highlighted in gray.

(c) Spatial organization of *LjVTI12* domains, shown to scale. The coiled-coil domain and the SNARE motif are connected by a 28 amino acid linker, and the SNARE motif and the transmembrane domain by a six amino acid linker. The same color code is used as in (b).

named *LjVTI12* (Figure 4b). The *LjVTI12* gene is 3441 bp long, and is divided into five exons and four introns (Figure S4). The encoded LjVTI12 protein is 221 amino acids long, and is predicted to have a molecular mass of 24.7 kDa. The highly conserved SNARE motif is 67 amino acids long (pink box in Figure 4b,c), and is proposed to act as a protein–protein interaction module in assembly of the SNARE protein complex. It is therefore considered to be essential for driving membrane fusion. The protein possesses a transmembrane domain (gray box in Figure 4b,c) and a long coiled-coil N-terminal region of 60 amino acids for interaction with other SNARE protein complex partners (yellow box in Figure 4b,c). Expression analysis of a chimeric gene encoding an N-terminal YFP fusion of the LjVTI12 protein under the control of the 2 kb *LjVTI12* promoter revealed a low expression level along the root epidermis, with activation of the promoter upon arbuscular mycorrhizal fungus colonization (Figure 5a–c).

In vivo subcellular localization of the fusion protein in mycorrhizal hairy roots was studied via confocal micro-

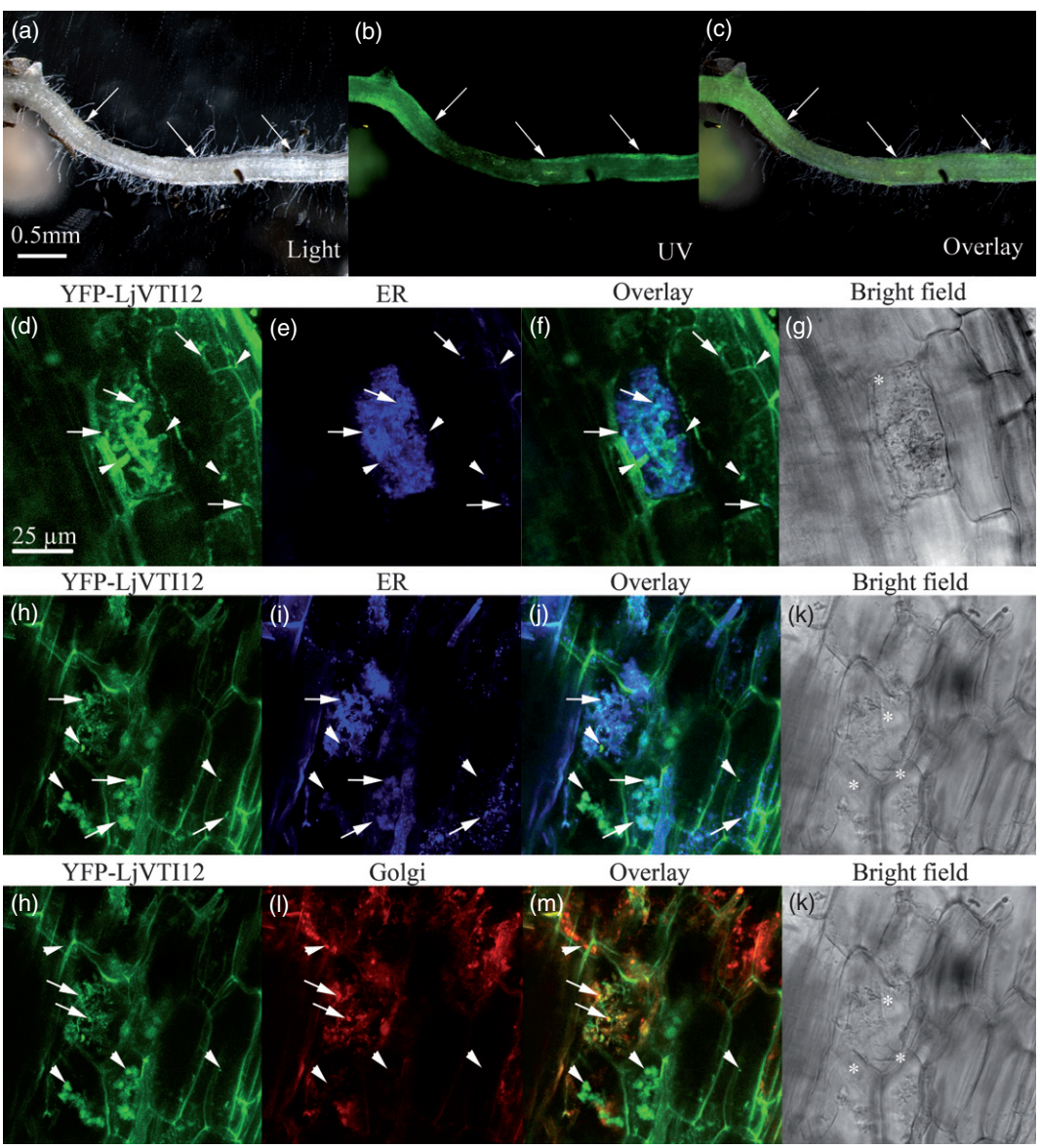

Figure 5. Spatial pattern of *LjVTI12* promoter activity and subcellular localization of YFP–LjVTI12 fusion protein in transgenic *Lotus* hairy roots.
(a–c) Promoter activity observed using a UV binocular microscope. Arrows indicate hyphal entry points.
(d–m) Laser scanning confocal microscopy indicating the subcellular localization of YFP–LjVTI12 protein [except bright-field micrographs in (g) and (k)]. (d, h) YFP–*LjVTI12* fusion protein localization; (e, i) labeled endoplasmic reticulum (ER), (l) labeled Golgi apparatus. (f, j, m) Merged images showing both green and blue (ER) or red (Golgi) fluorescence. Arrows point to fluorescence signals indicating localization of *LjVTI12* in ER or Golgi, respectively; arrowheads indicate LjVTI12, which does not localize to either ER or Golgi. The asterisks in (g) and (k) indicate cortex cells colonized by arbuscular mycorrhizal fungus.
Scale bars = 0.5 cm (a–c) and 25 μm (d–m).

scopy, and demonstrated localization of the protein to arbusculated cells, as well as dynamic intracellular structures co-localizing either with the ER or the Golgi apparatus. Those fluorescent signals, which did not co-localize with ER or Golgi markers, are suggested to be en route to other subcellular components (Figure 5d–m and Movie S1). Precise *in vivo* localization of LjVTI12–YFP was complicated due to the highly dynamic protein movement. Nevertheless, partial co-localization with the Golgi apparatus in the form of small punctate structures in arbusculated cells (see Figure 5m) is consistent with published work on post-Golgi localization of AtVTI12 (Uemura *et al.*, 2004). In accordance with the increased *LjVTI12* transcript levels in mycorrhizal roots (Table 2), the data suggest activation of *LjVTI12* expression in root cells containing arbuscules via arbuscule-specific signals.

In order to analyze whether the LjVTI12 protein is essential for AM symbiosis development, specific down-regulation of the expression of *LjVTI12* in *Lotus* roots using artificial microRNA (amiR) (Schwab *et al.*, 2006) was performed. The amiR targeted *LjVTI12* transcripts between bp 401 and 420 (Figure 6a and Figure S4). To ensure the specificity of the amiR, sequence comparison with the closest homologous transcript (*Lj050801.1*) was performed, and revealed crucial mismatches at the cleavage site between positions 10 and 11 (dashed lines, Figure 6a). The presence of these sites, no more than five mismatches in total and never two in a row, allowed correct target site recognition (Schwab *et al.*, 2005), thus excluding *Lj050801.1* as an alternative possible amiR target. The *LjVTI12* amiR DNA construct was expressed in hairy roots via *A. rhizogenes*-mediated gene transfer in combination with a constitutively expressed eGFP marker gene (Karimi *et al.*, 2002), allowing green fluorescent transgenic hairy roots expressing both GFP and the amiR to be distinguished from non-GFP expressing hairy roots and wild-type roots (GFP–) (Figure 6b). The *LjVTI12* transcript abundance was reduced up to fivefold in amiR roots compared to GFP– roots on three individual plants (amiR-1 to -3, Figure 7a), but *Lj050801.1* expression was unaffected, thus indicating gene-specific silencing of *LjVTI12*. Microscopic studies of Trypan blue-stained amiR roots revealed normal colonization rates with the AM fungus *G. intraradices* when compared to GFP– roots (Figure 6c). Moreover, the relative distribution of intra-radical fungal structures was unaffected in mycorrhizal amiR hairy roots compared with mycorrhizal wild-type (GFP–) roots (Figure 6c).

Intra-radical hyphae, hyphal coils and arbuscules are the site of nutrient exchange between plants and fungi (Karandashov *et al.*, 2004; Parniske, 2008). Thus, these structures were used as a qualitative marker for fungal health. The number of septa, which separate healthy and collapsed dead parts of fungal branches (Cox *et al.*, 1980), per unit root length remained unchanged in intra-radical hyphae of

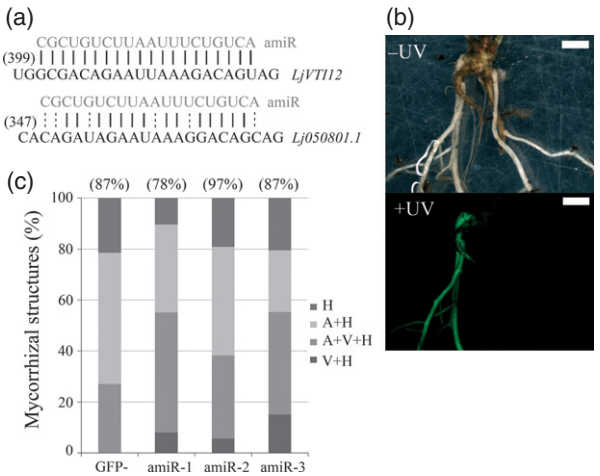

Figure 6. Artificial microRNA (amiR) targetting *LjVTI12* transcripts in *Lotus* hairy roots and quantitative effects on morphology of arbuscular mycorrhizal fungus structures.
(a) amiR target cleavage sequence and position (number in parentheses) on *LjVTI12* transcripts and the closest homolog *Lj050801.1*. Dashed lines represent improbable amiR binding.
(b) Chimeric *Lotus* root system (–UV) showing non-fluorescent wild-type roots (GFP–) and green fluorescent transgenic hairy roots expressing amiR (+UV) due to constitutively co-expressed eGFP. Scale bar = 5 mm.
(c) Mycorrhizal structures in GFP– and amiR roots of three independent biological replicates (amiR-1 to 3). H, hyphae; V, vesicle; A, arbuscule. The number in parentheses represents the overall colonization rate.

amiR roots compared to GFP– roots, suggesting a functional mycorrhiza (Figure 7b). Next, arbuscules in three composite plants containing amiR and GFP– hairy roots were classified into six size classes (Figure 7c). The amiR roots harbored significantly fewer arbuscules in the 30–45 μm class (except plant 1), as well as in the 45–60 μm class. On the other hand, significantly more arbuscules of size 15–30 μm developed in all amiR roots. We then qualitatively classified the arbuscular mycorrhizal fungus structures according to the presence and location of septa (Figure 7d) in and near arbuscules. Colonized GFP– roots showed more than 55% healthy fungal structures (class 1) lacking septa either in arbuscules or in hyphae attached to them. In the same GFP– roots, approximately 25% of observed arbuscules showed internal septa in fine hyphal branches (class 2), and approximately 20% of the collapsed arbuscules were separated by septa from the hyphal network (class 3) (Figure 7d). In all colonized amiR roots, reduced *LjVTI12* expression correlated with a significant shift of AM morphology from arbuscules of class 1 towards morphology classes 2 and 3, indicating a significantly reduced number of healthy fungal structures. A similar experiment was performed using well-colonized hairy roots transformed with an empty vector (EV) control (Figure S5). Analysis of the arbuscule morphology classes revealed a similar representation of classes 1–3 in GFP– and GFP+ EV-roots, respectively, to that in GFP– roots of composite plants with well-colonized amiR roots (Figure 7d).

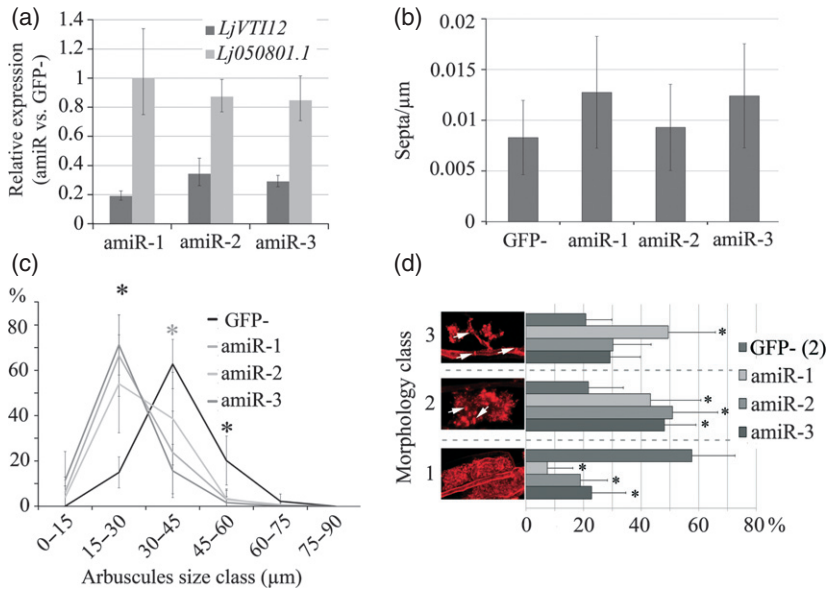

Figure 7. Gene expression of *LjVTI12* and *Lj050801.1 l* and mycorrhiza phenotype of *LjVTI12*-silenced *Lotus* hairy roots.
(a) Gene expression of *LjVTI12* and homolog *Lj050801.1* in mycorrhizal amiR roots relative to non-transgenic mycorrhizal GFP– roots.
(b) Number of septa counted in intra-radical mycorrhizal hyphae. Values are means ± SE of at least 10 infection sites (n = 3–11).
(c) Arbuscule size classes in silenced *Lotus* lines compared to GFP– control. Black asterisks indicate significant differences with a P value <0.05 for all three plants. The gray asterisk indicates significant differences with a P value <0.05, with the exception of plant amiR-2 (no statistical difference). Values are means ± SE of at least seven arbuscules ($n \geq 10$).
(d) Arbuscule morphology classes. Class 1 represents arbuscules with healthy morphology; classes 2 and 3 represent arbuscules exhibiting weak and strong degeneration, respectively. White arrows indicate hyphal septa or intra-arbuscular septa. Values are the percentage of at least four arbuscules ($n \geq 10$) ± SE. GFP – (2) indicates GFP– roots on the amiR-2 plant. Similar results were obtained with other amiR plants. Asterisks indicate significant differences with P value <0.05.

The occurrence of an increased number of small collapsed arbuscules with septa provided evidence for an essential role of the corresponding Qb-SNARE protein LjVTI12 in arbuscule maturation and senescence through control of intracellular trafficking, secretion and/or vesicular transport.

Overall, functional dissection of the mycorrhiza-inducible *StPT3* gene promoter (Rausch *et al.*, 2001) led to identification of two proximate CREs, CTTC and P1BS, that occur in the promoters of all mycorrhiza-specific Pi transporter genes investigated here. The CTTC motif was shown to be necessary and sufficient for mycorrhiza inducibility and Pi repression of AM-inducible Pi transporter genes. Moreover, co-occurrence and spatial localization of CTTC and P1BS suggested transcriptional control of mycorrhizal Pi uptake through interaction between independently evolved AM and Pi starvation response pathways that converge on promoters containing both CREs. Both sequence motifs were subsequently used in combination as a target for scanning the *Lotus* genome sequence. This approach revealed a set of candidate genes that are likely to be involved in AM symbiosome development, thus supporting our efforts to establish a functional gene atlas of the AM symbiosome in *L. japonicus*. Subsequent functional analysis of the vesicle-associated SNARE protein LjVTI12, in combination with LjVTI12 localization to the ER and Golgi complex, provided evidence in support of specific functions of SNARE proteins, and probably their interacting proteins, in AM symbiosis, extending beyond the conventional 'housekeeping' activities associated with vesicle trafficking. This function is supported by the recent identification of a VAMP72 protein from the R-SNARE family that is required for arbuscule development (Ivanov *et al.*, 2012). Future work will shed more light on mycorrhizal functions of core proteins of the trafficking pathway and their role in AM symbiosome development and functioning of the symbiosome in selective exchange of essential nutrients and metabolites with the mycoheterotroph.

EXPERIMENTAL PROCEDURES

Plant growth

Solanum tuberosum var. *Désirée* and *Lotus japonicus* var. *Gifu* were used for all experimental studies. Plants were cultivated in growth chambers (Percival, www.percival-scientific.com) with 16 h light (26°C)/8 h dark (22°C). For sterile growth conditions, *Lotus* seeds were scarified in sulfuric acid followed by surface sterilization (0.3% NaOCl, 0.1% SDS). Murashige and Skoog medium (Duchefa, www.duchefa.com) containing 10 or 20% sucrose was used as the substrate for *in vitro* culture of *Lotus* or potato plants, respectively. The mycorrhizal fungus *G. intraradices* BEG75 was mixed with a sterile sand/soil mixture (9:1) and used as a dry inoculum. Potato and *Lotus* plants were grown in the greenhouse and fertilized weekly over 6 weeks with half-strength Hoagland solution (Arnon and Hoagland,

1940) containing 5 μM Pi to establish low-Pi conditions. Reversion to high-Pi conditions comprised a shift to 1 and 5 mM Pi for potato and *Lotus*, respectively, for an additional 2 weeks of cultivation.

Histochemical staining and microscopy

Mycorrhizal structures were revealed using Trypan blue staining as described previously (Brundrett *et al.*, 1984). β-glucuronidase counter-staining was performed with samples of mycorrhizal plants as described previously (Karandashov *et al.*, 2004). For Wheat Germ Agglutinin (WGA) Alexa Fluor 594 staining (Life Technologies, www.lifetechnologies.com), roots were placed into phosphate-buffered saline containing 0.2 μg ml^{-1} WGA Alexa Fluor. ER-Tracker Blue-White DPX and BODIPY TR C5-Ceramide (Life Technologies, www.lifetechnologies.com) were used for ER and Golgi staining, respectively. A Leica TCS SPE confocal scanning microscope (Leica Microsystems, www.leica-microsystems.de) was used to visualize fluorescent signals. WGA Alexa Fluor, YFP, ER-Tracker and BODIPY TR C_5 ceramide were detected using 532/590–650 nm, 488/505–530 nm, 405/420–480 nm and 532/605–625 nm excitation/emission filters, respectively.

Production of potato and *Lotus* plants harboring transformed hairy roots

The production of hairy root composite *Lotus* plants was performed as previously described (Boisson-Dernier *et al.*, 2001) with minor changes. Sterile plant hypocotyls were infected with a needle dipped into an *A. rhizogenes* (ATCC 15843 strain) suspension (10 mM PIPES/KOH pH 6.8, 200 mM sorbitol) transformed with the plasmid of interest. Transgenic hairy roots were screened for fluorescence signal using a Leica MZ16F fluorescence binocular microscope. Plants with transformed roots were then transferred to the greenhouse and inoculated as described above.

DNA cloning

Truncated fragments of the *StPT3* promoter were amplified via PCR from genomic DNA of potato (Dellaporta *et al.*, 1983) using forward primers −1220-F, −1052-F, −640-F, −511-F, −298-F, −201-F or −135-F (Table S2) and the reverse primer END5+-R. The PCR products were inserted into pBluescript KS- (Agilent Technologies, www.genomics.agilent.com) containing the *GUS–nos* construct originating from the plasmid 5′*AKT1*-320.X (Lagarde *et al.*, 1996). The truncated promoter::*GUS-nos* constructs were sub-cloned into the binary vector BIN19 (Bevan, 1984) for *Agrobacterium* transformation. Primers 129-allmost-F, 129-motif1-F, 129–motif1,2-F and 129–motif1-3-F, respectively, were designed to amplify *StPT3* promoter truncations lacking motifs described in Karandashov *et al.* (2004), the TGTT motif, the AAAA motif and the TGCA motif, respectively. PCR using primers 129-bp-F and 129-bp-R amplified the 129 bp region between −640 and −511 upstream of the start ATG of *StPT3*, which was introduced into pBluescript SK- containing the CaMV 35S *minimal promoter::GUS-nos* construct (provided by Therese Mandel, Institute of Plant Sciences, University of Berne, Switzerland). The entire construct was excised from pBluescript SK- and sub-cloned into BIN 19. PCR using primers -mot5l-F and END5+-R was performed to generate a *StPT3* promoter fragment lacking the CTTC element (−535 to −525 bp upstream of the start ATG). Further PCRs using primers END5+-R and -mot5a-F, -mot3ext1-F, -mot3ext2-F and -mot3Sac-F were performed to extend the amplified region of the *StPT3* promoter to obtain a fragment from −640 to the start ATG lacking the CTTC element (−*CTTC*). The same method was repeated to amplify a *StPT3* promoter fragment from −640 to the start ATG lacking the ATAATA element (−523 to −517 bp upstream of the start ATG) by replacing the initial step with forward primer -mot5l-F with two PCR reactions with primers -mot6l-F and -mot6a-F, respectively (−*TAAT*). The −*CTTC* and −*TAAT* promoter fragments were cloned into pBluescript KS- containing the GUS–nos construct, and were subsequently sub-cloned into BIN 19. Primers 5′-AG-CCTCCACAAGCTTAACC-3′ and 5′-GCTCACAATACTGGCGTTCA-3′ were used to amplify the 2 kb promoter from *LjVTI12* for cloning into pGEM-T Easy (Promega, http://www.promega.de). The 35S CaMV promoter from the Gateway-compatible plasmid pENSG (Jakoby *et al.*, 2006) was replaced by the *LjVTI12* promoter. Primers 5′-ATGAGTAGTGTGTTCGAG-3′ and 5′-CTATTTCGAAAGTT-TAAAG-3′ were used to amplify the *LjVTI12* coding sequence from an *L. japonicus/G. intraradices* cDNA library. The PCR fragment was cloned into pGEMT-Easy and subsequently used as template for Gateway cloning, according to the Gateway technology manual (version E, 22 September 2003), http://pef.aibn.uq.edu.au/support/material/download/Gateway_Technology.pdf. pENSG carrying the *LjVTI12* promoter was used in the LR Gateway reaction to generate an N-terminal YFP–LjVTI12 fusion protein. The design and cloning of the amiRNA were performed as described at http://wmd3.weigelworld.org. Gateway recombination sites were added 5′ upstream and 3′ downstream of the amiRNA for cloning into the pH7WG2D plasmid via LR recombination Karimi *et al.* (2002). All plasmids were checked by DNA sequencing before transformation into micro-organisms or plants.

RNA extraction and quantitative RT-PCR

Total RNA was extracted from 150 mg root tissue according to manufacturer's instructions (Macherey Nagel GmbH & Co. KG, www.mn-net.com). RNA quantity and quality was checked using a NanoDrop 1000 spectrofluorometer (Thermo Scientific, www.thermoscientific.com). Total RNA (1 μg) was subjected to DNase treatment and checked by PCR for DNA contamination. RNA was reverse-transcribed to cDNA using poly(dT) as primer according to the manufacturer's instructions (Promega, www.promega.com). The final volume of dissolved cDNA was 100 μl. For quantitative RT-PCR, 1 μl cDNA was mixed with 10 μl Power SYBR Green RT-PCR Reagents Kit (Applied Biosystems, www.appliedbiosystems.com) and 10 pmol forward and reverse gene-specific primers (Table S2) in a final volume of 20 μl. PCR was run on an Applied Biosystems 7500 Real-Time PCR System. Analysis of relative gene expression was performed using the $2^{-\Delta\Delta_t^C}$ method, with *ubiquitin* as the endogenous reference gene.

Phylogenetic footprinting and promoter analysis

The following genes and promoters of previously described mycorrhiza-inducible Pi transporter genes, for which promoters were available, were used for phylogenetic footprinting analysis: *StPT3* (Rausch *et al.*, 2001), *StPT4* and *LePT4* (Rausch *et al.*, 2001; Nagy *et al.*, 2005), *PhPT3*, *4* and *5* (Wegmüller, 2008) and *MtPT4* (Harrison *et al.*, 2002). In addition, the promoters of the entire *Pht1* gene family of Arabidopsis (Mudge *et al.*, 2002) and rice, including the mycorrhiza-inducible *OsPT11* and *OsPT13* genes, (Paszkowski *et al.*, 2002) were manually extracted from the chromosome sequences found in the National Center for Biotechnology Information nucleotide database (http://www.ncbi.nlm.nih.gov/). The mycorrhiza-inducible genes encoding proteins other than Pi transporters were *PsENOD12b* (Scheres *et al.*, 1990; Govers *et al.*, 1991), *MtGST* (Krajinski *et al.*, 2003), *MtLec5* (Frenzel *et al.*, 2006) and *VfLB29* (Vieweg *et al.*, 2004;

Fehlberg *et al.*, 2005). The genes corresponding to the promoters were aligned using Clustal W (Thompson *et al.*, 1994) (using EMMA, a command line interface for ClustalW in the EMBOSS package, http://www.csc.fi/english/research/sciences/bioscience/programs/clustalw/index_html), and a maximum-parsimony phylogenetic tree was subsequently generated. Then bootstrap analysis (100 bootstraps) was performed using PHYLIP software (Felsenstein, 1995). This phylogenetic tree and the corresponding promoters were analyzed using FOOTPRINTER version 3.0 (Blanchette and Tompa, 2002). A thousand base pairs (or less, depending on sequence availability) of the sequences upstream of the initiator ATG were analyzed for motifs of 7–10 bp in length, allowing for two mismatches. Because less conserved and unrelated sequences were included in the query, regulatory element loss was set to the least possible penalty (0.5), and large sub-regions were chosen at the lowest cost (500–1000 bp sub-region, cost 0–0.5). Several combinations of the above-mentioned mycorrhiza-inducible Pi transporter genes in combination with the controls were tested, and the most conserved elements were merged by hand to produce Figure 2. Once motifs had been identified, the promoters were scanned manually to identify variations of the motifs. The identified motifs and the entire *StPT3* promoter sequence were scanned for homology with known *cis*-acting elements using the PLACE database (http://www.dna.affrc.go.jp/PLACE/info.html (Higo *et al.*, 1998) and the PlantCARE database (http://bioinformatics.psb.ugent.be/webtools/plantcare/html (Lescot *et al.*, 2002).

Gene enrichment analysis

A total of 31 208 *Lotus* genes were mapped onto Arabidopsis transcripts using reciprocal BLAST. Functional annotation of the Arabidopsis transcripts was adopted from Brautigam *et al.* (2011). The upstream sequence of each *Lotus* gene was scanned for the presence of the CTTC and P1BS elements, and the number of mismatches in each element was noted. This search yielded 4634 genes, of which 338 had one or fewer mismatches in both elements. If the presence of the elements had occurred by chance, it would be expected that each of the functional sub-groups would be represented within the sub-groups in similar percentages compared to the complete dataset. For each functional group, the proportion it covers in the whole dataset, the motif dataset with up to three mismatches allowed and the motif dataset with only one mismatch allowed were calculated (number of genes in the functional group divided by number of genes in the respective dataset). In a second step, the proportions of all genes in the functional class 'transport' were calculated based on the transport sub-groups.

Localization experiment in Arabidopsis leaf cells

Col-0 wild-type Arabidopsis plants grown in the greenhouse were transfected by particle bombardment with the respective constructs. For bombardment, 30 mg of gold particles (Bio-Rad, www.bio-rad.com) were incubated for 15 min with 1 ml of 70% v/v ethanol. The reaction tube was centrifuged, and particles were washed twice and resuspended in 1 ml of sterile water and briefly sonicated. Then 600 ng plasmid were added to a reaction tube to a final volume of 12 μl, and 20 μl of 2.5 M $CaCl_2$, 8 μl of 0.1 M spermidine and 10 μl of the gold particle solution were added and vortexed for 10 min. Gold particles were then washed with 100 μl of 70% v/v ethanol and 40 μl absolute ethanol. Finally, the gold particles were resupended in 24 μl absolute ethanol by sonication. Two aliquots (10 μl) were spotted onto a macro carrier plate (Bio-Rad) and dried by evaporation. Particle bombardment was performed using a Helios helium gun (Bio-Rad) according to the manufacturer's instructions. Arabidopsis plants were kept in darkness for 24 h prior to microscopic observation. A Leica DMRB fluorescence microscope and appropriate filters were used to visualize fluorescent signals.

ACKNOWLEDGEMENTS

We are grateful to M'Barek Tamasloukht (Institute of Agricultural Sciences, Federal Institute of Technology Zurich, Switzerland) for his initial support of the work on the CTTC motif. We thank Alban Jacques and Paul Schulze-Lefert (Max Planck Institute for Plant Breeding Research, Cologne, Germany) for fruitful discussions during the course of our work. We thank Karl Pioch and the reviewers for their careful reading of the manuscript. This work was supported in part by Priority Program 1212 of the Deutsche Forschungsgemeinschaft and the Swiss National Science Foundation (grant number 3100A0-109618 to M.B.).

SUPPORTING INFORMATION

Additional Supporting Information may be found in the online version of this article.

Figure S1. *StPT3* promoter sequence analysis.

Figure S2. *StPT3* promoter deletion constructs and their activity in stably transformed mycorrhizal potato roots.

Figure S3. Qualitative GUS analysis in *ΔCTTC-promStPT3::GUS* and *promStPT3::GUS* lines.

Figure S4. Gene structure of *LjVTI12* showing the presence of five exons.

Figure S5. *LjVTI12* and *Lj050801.1* expression and mycorrhiza phenotype in *Lotus* hairy roots carrying empty vector (EV).

Table S1. List of *Lotus* genes containing both CREs analyzed by quantitative RT-PCR.

Table S2. Primers used for cloning and quantitative RT-PCR.

Movie S1. Dynamic intracellular movement of eGFP–LjVTI12 fusion protein in Arabidopsis leaf epidermis cell.

REFERENCES

Alexander, T., Toth, R., Meier, R. and Weber, H.C. (1989) Dynamics of arbuscule development and degeneration in onion, bean, and tomato with reference to vesicular arbuscular mycorrhizae in grasses. *Can. J. Bot.* **67**, 2505–2513.

Arnon, D.I. and Hoagland, D.R. (1940) Crop production in artificial culture solutions and in soils with special reference to factors influencing yields and absorption of inorganic nutrients. *Soil Sci.* **50**, 463–485.

Benfey, P.N., Ren, L. and Chua, N.H. (1989) The CaMV 35S enhancer contains at least two domains which can confer different developmental and tissue-specific expression patterns. *EMBO J.* **8**, 2195–2202.

Bevan, M. (1984) Binary *Agrobacterium* vectors for plant transformation. *Nucleic Acids Res.* **12**, 8711–8722.

Blanchette, M. and Tompa, M. (2002) Discovery of regulatory elements by a computational method for phylogenetic footprinting. *Genome Res.* **12**, 739–748.

Boisson-Dernier, A., Chabaud, M., Garcia, F., Becard, G., Rosenberg, C. and Barker, D.G. (2001) *Agrobacterium rhizogenes*-transformed roots of *Medicago truncatula* for the study of nitrogen-fixing and endomycorrhizal symbiotic associations. *Mol. Plant Microbe Interact.* **14**, 695–700.

Brautigam, A., Kajala, K., Wullenweber, J. *et al.* (2011) An mRNA blueprint for C4 photosynthesis derived from comparative transcriptomics of closely related C3 and C4 species. *Plant Physiol.* **155**, 142–156.

Breuillin, F., Schramm, J., Hajirezaei, M. *et al.* (2010) Phosphate systemically inhibits development of arbuscular mycorrhiza in *Petunia hybrida* and represses genes involved in mycorrhizal functioning. *Plant J.* **64**, 1002–1017.

Brundrett, M.C., Piche, Y. and Peterson, R.L. (1984) A new method for observing the morphology of vesicular–arbuscular mycorrhizae. *Can. J. Bot.* **62**, 2128–2134.

Bucher, M. (2007) Functional biology of plant phosphate uptake at root and mycorrhiza interfaces. *New Phytol.* **173**, 11–26.

Bucher, M., Wegmueller, S., Svistoonoff, S., Reinhardt, D., Stuurman, J. and Amrhein, N. (2008) A transgenic *dTph1* insertional mutagenesis system for forward genetics in mycorrhizal phosphate transport of *Petunia*. *Plant J.* **54**, 1115–1127.

Chen, A.Q., Gu, M.A., Sun, S.B., Zhu, L.L., Hong, S.A. and Xu, G.H. (2011) Identification of two conserved *cis*-acting elements, MYCS and P1BS, involved in the regulation of mycorrhiza-activated phosphate transporters in eudicot species. *New Phytol.* **189**, 1157–1169.

Cox, G., Moran, K.J., Sanders, F., Nockolds, C. and Tinker, P.B. (1980) Translocation and transfer of nutrients in vesicular–arbuscular mycorrhizas. III. Polyphosphate granules and phosphorus translocation. *New Phytol.* **84**, 649–659.

Dellaporta, S., Wood, J. and Hicks, J. (1983) A plant DNA minipreparation: version II. *Plant Mol. Biol. Rep.* **1**, 19–21.

Drissner, D., Kunze, G., Callewaert, N., Gehrig, P., Tamasloukht, M., Boller, T., Felix, G., Amrhein, N. and Bucher, M. (2007) Lyso-phosphatidylcholine is a signal in the arbuscular mycorrhizal symbiosis. *Science*, **318**, 265–268.

Elghachtouli, N., Paynot, M., Morandi, D., Martintanguy, J. and Gianinazzi, S. (1995) The effect of polyamines on endomycorrhizal infection of wild-type *Pisum sativum*, cv. Frisson (nod^+myc^+) and two mutants (nod^-myc^+ and nod^-myc^-). *Mycorrhiza*, **5**, 189–192.

Fehlberg, V., Vieweg, M.F., Dohmann, E.M., Hohnjec, N., Puhler, A., Perlick, A.M. and Kuster, H. (2005) The promoter of the leghaemoglobin gene *VfLb29*: functional analysis and identification of modules necessary for its activation in the infected cells of root nodules and in the arbuscule-containing cells of mycorrhizal roots. *J. Exp. Bot.* **56**, 799–806.

Felsenstein, J. (1995) PHYLIP (Phylogeny Inference Package) version 3.6. *Cladistics*, **5**, 164–166.

Frenzel, A., Tiller, N., Hause, B. and Krajinski, F. (2006) The conserved arbuscular mycorrhiza-specific transcription of the secretory lectin MtLec5 is mediated by a short upstream sequence containing specific protein binding sites. *Planta*, **224**, 792–800.

Genre, A., Chabaud, M., Timmers, T., Bonfante, P. and Barker, D.G. (2005) Arbuscular mycorrhizal fungi elicit a novel intracellular apparatus in *Medicago truncatula* root epidermal cells before infection. *Plant Cell*, **17**, 3489–3499.

Govers, F., Harmsen, H., Heidstra, R., Michielsen, P., Prins, M., van Kammen, A. and Bisseling, T. (1991) Characterization of the pea ENOD12B gene and expression analyses of the two ENOD12 genes in nodule, stem and flower tissue. *Mol. Gen. Genet.* **228**, 160–166.

Guether, M., Balestrini, R., Hannah, M., He, J., Udvardi, M.K. and Bonfante, P. (2009) Genome-wide reprogramming of regulatory networks, transport, cell wall and membrane biogenesis during arbuscular mycorrhizal symbiosis in *Lotus japonicus*. *New Phytol.* **182**, 200–212.

Hamel, C., Liu, A., Hamilton, R.I., Ma, B.L. and Smith, D.L. (2000) Acquisition of Cu, Zn, Mn and Fe by mycorrhizal maize (*Zea mays* L.) grown in soil at different P and micronutrient levels. *Mycorrhiza*, **9**, 331–336.

Hansen, A.C., Busk, H., Marcker, A., Marcker, K.A. and Jensen, E.O. (1999) VsENBP1 regulates the expression of the early nodulin PsENOD12B. *Plant Mol. Biol.* **40**, 495–506.

Hardham, A.R., Jones, D.A. and Takemoto, D. (2007) Cytoskeleton and cell wall function in penetration resistance. *Curr. Opin. Plant Biol.* **10**, 342–348.

Harrison, M.J., Dewbre, G.R. and Liu, J. (2002) A phosphate transporter from *Medicago truncatula* involved in the acquisition of phosphate released by arbuscular mycorrhizal fungi. *Plant Cell*, **14**, 2413–2429.

Harrison, M.J., Liu, J.Y., Blaylock, L.A., Endre, G., Cho, J., Town, C.D. and VandenBosch, K.A. (2003) Transcript profiling coupled with spatial expression analyses reveals genes involved in distinct developmental stages of an arbuscular mycorrhizal symbiosis. *Plant Cell*, **15**, 2106–2123.

Harrison, M.J., Pumplin, N., Mondo, S.J., Topp, S., Starker, C.G. and Gantt, J.S. (2010) *Medicago truncatula* Vapyrin is a novel protein required for arbuscular mycorrhizal symbiosis. *Plant J.* **61**, 482–494.

Hause, B., Mrosk, C., Forner, S., Hause, G., Kuster, H. and Kopka, J. (2009) Composite *Medicago truncatula* plants harbouring *Agrobacterium rhizogenes*-transformed roots reveal normal mycorrhization by *Glomus intraradices*. *J. Exp. Bot.* **60**, 3797–3807.

Higo, K., Ugawa, Y., Iwamoto, M. and Higo, H. (1998) PLACE: a database of plant *cis*-acting regulatory DNA elements. *Nucleic Acids Res.* **26**, 358–359.

Ivanov, S., Fedorova, E. and Bisseling, T. (2010) Intracellular plant microbe associations: secretory pathways and the formation of perimicrobial compartments. *Curr. Opin. Plant Biol.* **13**, 372–377.

Ivanov, S., Fedorova, E.E., Limpens, E., De Mita, S., Genre, A., Bonfante, P. and Bisseling, T. (2012) Rhizobium–legume symbiosis shares an exocytotic pathway required for arbuscule formation. *Proc. Natl Acad. Sci. USA*, **109**, 8316– 8321.

Jakoby, M.J., Weinl, C., Pusch, S., Kuijt, S.J.H., Merkle, T., Dissmeyer, N. and Schnittger, A. (2006) Analysis of the subcellular localization, function, and proteolytic control of the Arabidopsis cyclin-dependent kinase inhibitor ICK1/KRP1. *Plant Physiol.* **141**, 1293–1305.

Karandashov, V., Nagy, R., Wegmuller, S., Amrhein, N. and Bucher, M. (2004) Evolutionary conservation of a phosphate transporter in the arbuscular mycorrhizal symbiosis. *Proc. Natl Acad. Sci. USA*, **101**, 6285–6290.

Karimi, M., Inze, D. and Depicker, A. (2002) GATEWAY vectors for *Agrobacterium*-mediated plant transformation. *Trends Plant Sci.* **7**, 193–195.

Kloppholz, S., Kuhn, H. and Requena, N. (2011) A secreted fungal effector of *Glomus intraradices* promotes symbiotic biotrophy. *Curr. Biol.* **21**, 1204–1209.

Krajinski, F., Wulf, A., Manthey, K., Doll, J., Perlick, A.M., Linke, B., Bekel, T., Meyer, F., Franken, P. and Kuster, H. (2003) Transcriptional changes in response to arbuscular mycorrhiza development in the model plant *Medicago truncatula*. *Mol. Plant Microbe Interact.* **16**, 306–314.

Kwon, C., Neu, C., Pajonk, S. *et al.* (2008) Co-option of a default secretory pathway for plant immune responses. *Nature*, **451**, 835–840.

Lagarde, D., Basset, M., Lepetit, M., Conejero, G., Gaymard, F., Astruc, S. and Grignon, C. (1996) Tissue-specific expression of *Arabidopsis* AKT1 gene is consistent with a role in K^+ nutrition. *Plant J.* **9**, 195–203.

Lescot, M., Dehais, P., Thijs, G., Marchal, K., Moreau, Y., Van de Peer, Y., Rouze, P. and Rombauts, S. (2002) PlantCARE, a database of plant *cis*-acting regulatory elements and a portal to tools for *in silico* analysis of promoter sequences. *Nucleic Acids Res.* **30**, 325–327.

Limpens, E., Ramos, J., Franken, C., Raz, V., Compaan, B., Franssen, H., Bisseling, T. and Geurts, R. (2004) RNA interference in *Agrobacterium rhizogenes*-transformed roots of *Arabidopsis* and *Medicago truncatula*. *J. Exp. Bot.* **55**, 983–992.

Moreno-Hagelsieb, G. and Latimer, K. (2008) Choosing BLAST options for better detection of orthologs as reciprocal best hits. *Bioinformatics*, **24**, 319–324.

Mudge, S.R., Rae, A.L., Diatloff, E. and Smith, F.W. (2002) Expression analysis suggests novel roles for members of the Pht1 family of phosphate transporters in *Arabidopsis*. *Plant J.* **31**, 341–353.

Nagy, R., Karandashov, V., Chague, V., Kalinkevich, K., Tamasloukht, M., Xu, G., Jakobsen, I., Levy, A.A., Amrhein, N. and Bucher, M. (2005) The characterization of novel mycorrhiza-specific phosphate transporters from *Lycopersicon esculentum* and *Solanum tuberosum* uncovers functional redundancy in symbiotic phosphate transport in solanaceous species. *Plant J.* **42**, 236–250.

Nagy, R., Drissner, D., Amrhein, N., Jakobsen, I. and Bucher, M. (2009) Mycorrhizal phosphate uptake pathway in tomato is phosphorus-repressible and transcriptionally regulated. *New Phytol.* **181**, 950–959.

Osbourn, A., Field, B. and Jordan, F. (2006) First encounters – deployment of defence-related natural products by plants. *New Phytol.* **172**, 193–207.

Paradi, I., Bratek, Z. and Lang, F. (2003) Influence of arbuscular mycorrhiza and phosphorus supply on polyamine content, growth and photosynthesis of *Plantago lanceolata*. *Biol. Plant.* **46**, 563–569.

Parniske, M. (2008) Arbuscular mycorrhiza: the mother of plant root endosymbioses. *Nat. Rev. Microbiol.* **6**, 763–775.

Paszkowski, U., Kroken, S., Roux, C. and Briggs, S.P. (2002) Rice phosphate transporters include an evolutionarily divergent gene specifically activated in arbuscular mycorrhizal symbiosis. *Proc. Natl Acad. Sci. USA*, **99**, 13324–13329.

Pearson, W.R., Wood, T., Zhang, Z. and Miller, W. (1997) Comparison of DNA sequences with protein sequences. *Genomics*, **46**, 24–36.

Rausch, C., Daram, P., Brunner, S., Jansa, J., Laloi, M., Leggewie, G., Amrhein, N. and Bucher, M. (2001) A phosphate transporter expressed in arbuscule-containing cells in potato. *Nature*, **414**, 462–470.

Redecker, D., Kodner, R. and Graham, L.E. (2000) Glomalean fungi from the Ordovician. *Science*, **289**, 1920–1921.

Remy, W., Taylor, T.N., Hass, H. and Kerp, H. (1994) Four hundred-million-year-old vesicular arbuscular mycorrhizae. *Proc. Natl Acad. Sci. USA*, **91**, 11841–11843.

Rubio, V., Linhares, F., Solano, R., Martin, A.C., Iglesias, J., Leyva, A. and Paz-Ares, J. (2001) A conserved MYB transcription factor involved in phosphate starvation signaling both in vascular plants and in unicellular algae. *Genes Dev.* **15**, 2122–2133.

Sato, S., Nakamura, Y., Kaneko, T. *et al.* (2008) Genome structure of the legume, *Lotus japonicus*. *DNA Res.* **15**, 227–239.

Scheres, B., Van De Wiel, C., Zalensky, A. *et al.* (1990) The *ENOD12* gene product is involved in the infection process during the pea–*Rhizobium* interaction. *Cell*, **60**, 281–294.

Schwab, R., Palatnik, J.F., Riester, M., Schommer, C., Schmid, M. and Weigel, D. (2005) Specific effects of microRNAs on the plant transcriptome. *Dev. Cell*, **8**, 517–527.

Schwab, R., Ossowski, S., Riester, M., Warthmann, N. and Weigel, D. (2006) Highly specific gene silencing by artificial microRNAs in *Arabidopsis*. *Plant Cell*, **18**, 1121–1133.

Surpin, M., Zheng, H., Morita, M.T. *et al.* (2003) The VTI family of SNARE proteins is necessary for plant viability and mediates different protein transport pathways. *Plant Cell*, **15**, 2885–2899.

Thompson, J.D., Higgins, D.G. and Gibson, T.J. (1994) CLUSTAL W: improving the sensitivity of progressive multiple sequence alignment through sequence weighting, position-specific gap penalties and weight matrix choice. *Nucleic Acids Res.* **22**, 4673–4680.

Uemura, T., Ueda, T., Ohniwa, R.L., Nakano, A., Takeyasu, K. and Sato, M.H. (2004) Systematic analysis of SNARE molecules in *Arabidopsis*: dissection of the post-Golgi network in plant cells. *Cell Struct. Funct.* **29**, 49–65.

Ungar, D. and Hughson, F.M. (2003) SNARE protein structure and function. *Annu. Rev. Cell Dev. Biol.* **19**, 493–517.

Vieweg, M.F., Fruhling, M., Quandt, H.J., Heim, U., Baumlein, H., Puhler, A., Kuster, H. and Perlick, A.M. (2004) The promoter of the *Vicia faba* L. leghemoglobin gene *VfLb29* is specifically activated in the infected cells of root nodules and in the arbuscule-containing cells of mycorrhizal roots from different legume and nonlegume plants. *Mol. Plant Microbe Interact.* **17**, 62–69.

Wegmüller, S. (2008) *Regulatory mechanisms in mycorrhizal phosphate transport in Solanaceae*. PhD Thesis. Eidgenössische Technische Hoch-schule, ETH E–Collection Number 17416. ETH Bibliothek, ETH Zurich.

